IJP: Drugs and Drug Resistance 8 (2018) 312–319

Contents lists available at ScienceDirect

IJP: Drugs and Drug Resistance

journal homepage: www.elsevier.com/locate/ijpddr

The transcription factor SKN-1 and detoxification gene *ugt-22* alter albendazole efficacy in *Caenorhabditis elegans*

Pauline Fontaine, Keith Choe*

Department of Biology, University of Florida, Gainesville, FL 32611, USA

ARTICLE INFO

Keywords:
Detoxification
Albendazole
Drug resistance
Parasite
Anthelmintic

ABSTRACT

Parasitic nematodes infect over 1/4 th of the human population and are a major burden on livestock and crop production. Benzimidazole class anthelmintics are widely used to treat infections, but resistance is a widespread problem. Mutation of genes encoding the benzimidazole target β-tubulin is a well-established mechanism of resistance, but recent evidence suggests that metabolism of the drugs may also occur. Our objective was to investigate contributions of the detoxification-response transcription factor SKN-1 to anthelmintic drug resistance using *C. elegans*. We find that *skn-1* mutations alter EC_{50} of the common benzimidazole albendazole in motility assays by 1.5–1.7 fold. We also identify *ugt-22* as a detoxification gene associated with SKN-1 that influences albendazole efficacy. Mutation and overexpression of *ugt-22* alter albendazole EC_{50} by 2.3–2.5-fold. The influence of a nematode UGT on albendazole efficacy is consistent with recent studies demonstrating glucose conjugation of benzimidazoles.

1. Introduction

Parasitic nematodes infect a fourth of the world's human population (Caffrey, 2012) causing high global morbidity and mortality (Pullan et al., 2014; Torgerson et al., 2015). They also threaten agricultural and companion animals, as well as crop production causing over $100 billion losses in crop yield per year (Jasmer et al., 2003). Control of parasitic worms relies mainly on the use of a few major classes of anthelmintics, including macrocyclic lactones, imidazothiazoles, tetrahydropyrimidimes, and benzimidazoles. Benzimidazoles are the most widely used anthelmintics, with albendazole being recommended by the World Health Organization for community-wide treatment for soil-transmitted helminthiases (Anderson et al., 2014). By binding to β-tubulin BEN-1, and inhibiting microtubule polymerization (Lacey, 1990), benzimidazole drugs impair many processes in the model nematode *Caenorhabditis elegans* including body morphology and motility (Driscoll et al., 1989; Holden-Dye and Walker, 2014; Spence et al., 1982).

Nematodes have now evolved resistance to most anthelmintics, threatening sustainable control in agriculture and humans. Resistance to all three major classes of anthelmintics has been documented in parasitic nematodes and multidrug resistance can evolve in *C. elegans* under anthelmintic selection (Garcia et al., 2016; James and Davey, 2009; Ramos et al., 2016). Benzimidazole resistance is the most widespread, has been the most studied at the molecular level (Furtado et al., 2016), and resistance is emerging in human parasites (Krucken et al., 2017; Soukhathammavong et al., 2012; Vercruysse et al., 2011). Two general mechanisms have been shown to be associated with anthelmintic resistance. Mutations in genes encoding drug targets, including the benzimidazole β-tubulin target (Lacey, 1990), confer strong resistance in *C. elegans* (Driscoll et al., 1989; Lewis et al., 1980) and parasitic nematodes (Furtado et al., 2016). Evidence for anthelmintic drug biotransformation has also been accumulating recently (James and Davey, 2009; Vokral et al., 2012, 2013).

Detoxification of exogenous small molecules is a conserved metabolic process that occurs in three inter-dependent phases. In phase I, the drug is modified to introduce or reveal hydrophilic groups, which serve as anchors for phase II conjugation reactions to water-soluble moieties such as glucose and glutathione. The resulting conjugated metabolite is then pumped out of cells by phase III transporter proteins. Phase I enzymes include cytochrome P450s (CYPs) and short-chain dehydrogenases/reductases, and phase II reactions involve glutathione-S-transferases (GSTs) and UDP-glycosyltransferases (UGTs). Phase III ATP-binding cassette (ABC) transporters are efflux pumps. Benzimidazole resistance has been shown to be associated with increased expression or activity of detoxification genes and enzymes in free-living and parasitic nematodes (Jones et al., 2015; Vokral et al., 2012, 2013). However, genetic and molecular determinants of benzimidazole anthelmintic biotransformation remain largely unknown in nematodes.

* Corresponding author. Department of Biology and Genetics Institute, University of Florida, Newell Drive, Gainesville, FL 32611, USA.
E-mail address: kchoe@ufl.edu (K. Choe).

https://doi.org/10.1016/j.ijpddr.2018.04.006
Received 22 January 2018; Received in revised form 18 April 2018; Accepted 22 April 2018
Available online 25 April 2018

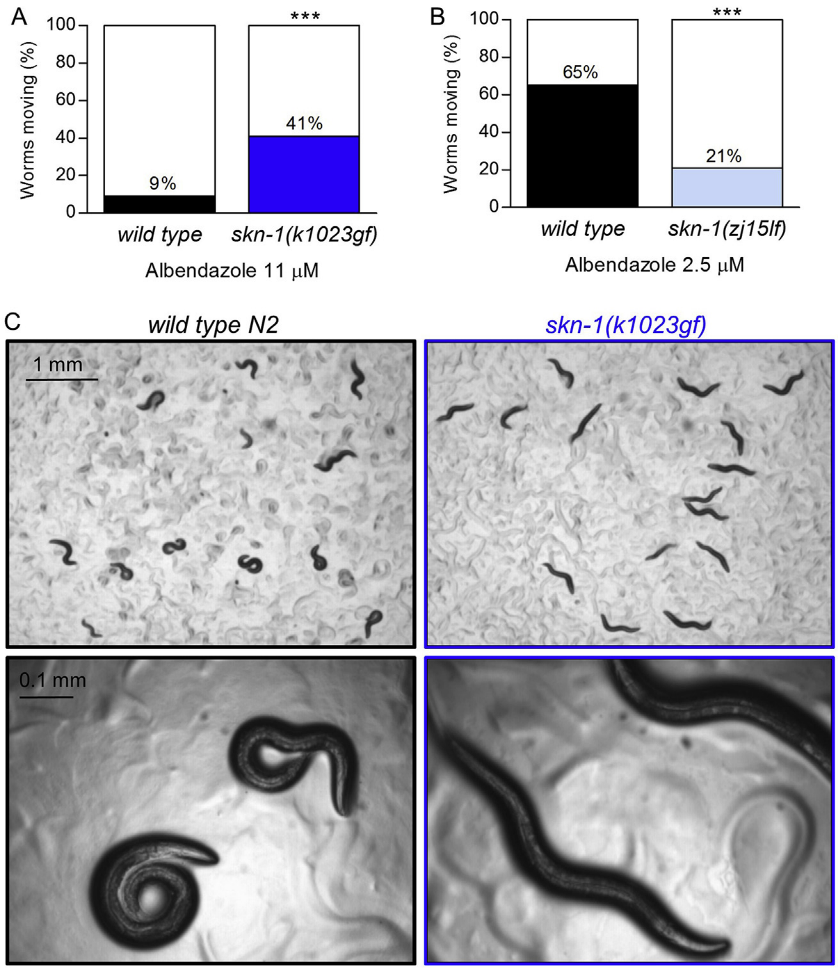

Fig. 1. *skn-1* mutations alter albendazole efficacy. (A) Percent long-term spontaneous motility of adult *wild type* N2 and *skn-1(k1023gf) (gf,* gain-of-function) worms exposed to 11 µM albendazole for 3 days. (B) Percent long-term spontaneous motility of adult *wild type* N2 and *skn-1(zj15lf)* (*lf*, loss-of-function) worms exposed to 2.5 µM albendazole for 3 days. (A and B) $n > 150$ worms per strain. ***$P < 0.001$ by Chi-square analysis. (C) *Wild type* N2 and *skn-1(k1023gf)* worms after 3 days on albendazole 11 µM plates.

The cap-n-collar (CNC) protein SKN-1 belongs to a family of basic region leucine zipper (bZIP) transcription factors that regulate expression of xenobiotic detoxification genes in *C. elegans*, *Drosophila,* and mammals (An and Blackwell, 2003; Choe et al., 2012). In *C. elegans,* SKN-1 promotes resistance to pro-oxidants and electrophiles by regulating numerous genes predicted to promote glutathione synthesis and small molecule detoxification (Choe et al., 2009, 2012; Oliveira et al., 2009; Park et al., 2009; Peddibhotla et al., 2015; Tang and Choe, 2015). SKN-1 homologs are found throughout the nematode phylum (Choe et al., 2012), but no studies have investigated them in the context of anthelmintics.

The free-living nematode *C. elegans* has been used to identify molecular targets of anthelmintics, functionally characterize drug targets, and identify molecular mechanisms of resistance (Driscoll et al., 1989; Janssen et al., 2013; Keiser, 2015). Using genetic manipulations in *C. elegans*, we show that SKN-1 influences efficacy of the common benzimidazole albendazole. Genetic manipulation of a detoxification gene associated with SKN-1 activation, *ugt-22,* also influences efficacy of albendazole. UGT-22 belongs to a group of rapidly evolving and expanding UGT protein family members that is shared with the clade V intestinal parasite *Haemonchus contortus*.

2. Materials and methods

2.1. *C. elegans* strains used

The following previously prepared strains were used: *wild type* N2 Bristol, QV212 *skn-1(k1023)*, QV225 *skn-1(zj15)*, CB3474 *ben-1(e1880)*, VC30084 *ugt-22(gk411724) IV*, and DR107 *unc-26(e205);dpy-4(e1166)* IV. The following transgenic lines were generated: QV303 *qvEx132*, QV304 *qvEx133*, and QV311 *qvEx140* were injected with [*ugt-22p::ugt-22 gDNA::ugt-22 3′UTR*; *myo-2p::tdTomato*; pGC31]. QV302 *qvEX131*, QV305 *qvEx134*, and QV306 *qvEx135* were injected with [*myo-2p::tdTomato*; pGC31]. QV308 *ugt-22(gk411724)*; *qvEx137*, QV309 *ugt-22(gk411724);qvEx138*, and QV312 *ugt-22(gk411724)*; *qvEx141* were injected with [*ugt-22p::ugt-22 gDNA:ugt-22* 3′UTR; *myo-2p::tdTomato*; pGC31]. Worms were cultured at 20 °C (Brenner, 1974) unless otherwise stated. Table S1 lists the names, alleles, and functions of all strains used in the present study.

2.2. Outcrossing of *ugt-22(gk411724)*

A million mutation project *ugt-22(gk411724)* IV allele carrying a nonsense mutation was outcrossed five times to DR107 *unc-26(e205);dpy-4(e1166)* IV resulting in strain QV300 *ugt-22(gk411724)*, sometimes referred to as *ugt-22(gk411724lf)* mutant worms for simplicity. Homozygosity was verified by restriction digestion and sequencing

A

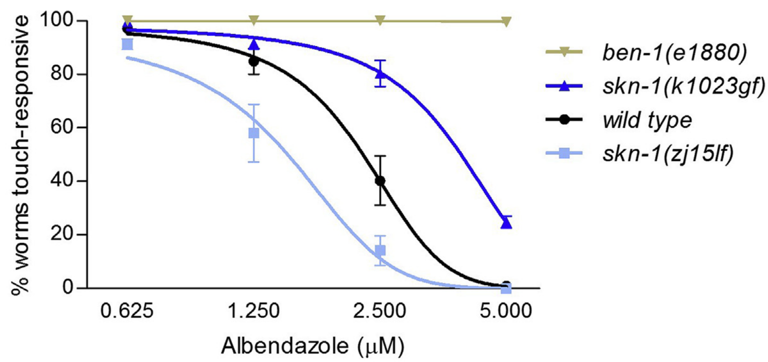

B

Strain	EC50, [μM] (95% CI)	*P* value	Fold change of EC50 from *wild type*	R^2
skn-1(zj15lf)	1.38 (1.21-1.58)	<0.001	- 1.6	0.911
wild type	2.18 (1.93-2.47)	-	-	0.845
skn-1(k1023gf)	3.67 (3.40-4.95)	<0.001	1.7	0.945

EC_{50} - 50% effective concentration
CI - confidence interval

Fig. 2. Albendazole dose-response curves are affected by *skn-1* mutations. (A) Percent rapid touch-responsive motility of adult *skn-1(zj15lf)* (*lf*, loss-of-function), *wild type* N2, *skn-1(k1023gf)* (*gf*, gain-of-function), and *ben-1(e1880)* worms exposed to albendazole for 3 days. (B) EC_{50} values, *P* values, and EC_{50} fold changes. Replicates equal 2–10 independent trials of ~50–60 worms per trial.

of a genomic PCR fragment.

2.3. Generation of transgenic worms

Overexpression of *ugt-22* and rescue of *ugt-22(gk411724lf)* mutant worms were achieved by amplifying the *ugt-22* gene sequence and 1340 bp upstream and 648 bp downstream from start and stop codons, respectively, from *wild type* N2 worm genomic DNA by PCR. The PCR product was injected into *wild type* N2 and *ugt-22(gk411724lf)* mutant worms at 25 ng/μl with *Pmyo2::tdTomato* (2 ng/μl) as a co-marker and plasmid pGC31 (81.22 ng/μl) as filler DNA. *Pmyo2::tdTomato* was used as a co-injection marker to confirm successful injection and isolate transgenic worms.

2.4. RNAi

RNAi was performed by feeding worms a strain of *Escherichia coli* [HT115(DE3)] that is engineered to transcribe double-stranded RNA (dsRNA) homologous to a target gene (Kamath et al., 2001). Bacteria with plasmid pPD129.36 were used as a control for nonspecific RNAi effects. RNAi was performed as described previously (Choe et al., 2009) with agar nematode growth medium (NGM) plates containing 0.2% β-lactose.

2.5. Motility assays

In all albendazole bioassays, worms were synchronized to the L1 larval stage by hypochlorite isolation of eggs and overnight starvation. L1 larvae were transferred to agar NGM plates containing albendazole. A minimum of three independent trials were performed for all motility assays except for *ben-1(e1880)* worms, which had essentially no response to albendazole. Dimethyl sulfoxide (DMSO) was used as vehicle control (final concentration was 0.20–0.44%) in all phenotypic bioassays using albendazole dissolved in this solvent.

Long-term spontaneous motility was assessed in adult worms after 3 days of growth over a 1 min 45 s time interval by recording videos with a Zeiss Discovery V12 microscope fitted with a OptixCam Summit Series camera. Videos were analyzed manually, and worms were categorized as ‘moving’ when they traveled at least one worm body length. Between 60 and 100 worms were scored per trial. Final concentrations of 2.5 or 11.0 μM albendazole were added just before pouring agar. These assay parameters were chosen because they resulted in a fraction (9–65%) of *wild type* N2 worms scored as moving allowing us to detect increases or decreases.

Rapid touch response was measured in adults after 3 days of growth by stroking worms once with an eyebrow hair pick along the posterior pharynx bulb, as described previously (Hart, 2006). A worm was scored positive if it reversed direction and moved backward at least one pharynx length immediately after stimulation (1–2 s). Dose-response curves were generated from all trials as described below under statistical analyses. Between 50 and 60 worms were scored per trial. As in the long-term motility bioassays, albendazole was mixed with the agar right before pouring to final concentrations of 0–5 μM.

2.6. Quantitative real-time PCR

Quantitative real-time PCR (qPCR) was used to quantify mRNA levels in L4 larvae to young adult stage worms under basal conditions or fed with appropriate dsRNA clones as described previously with some modifications (Choe et al., 2009). RNA was released from 10 individual worms with proteinase K (Ly et al., 2015), treated with dsDNase (37 °C for 2 min followed by 85 °C for 2 min) (Thermo Scientific), and cDNA was synthesized from worm lysate with the GoTaq 2-Step RT-qPCR System (Promega) according to the manufacturer's protocol. qPCR was performed in 10 μl reactions in a Realplex ep gradient S Mastercycler (Eppendorf) with GoTaq Green Master Mix (Promega) following the manufacturer's instructions. Data was analyzed using the standard curve method, with the housekeeping gene *rpl-2* as a reference control. Primer sequences are available on request.

2.7. Phylogenetic analyses

Homologs of UGT-22 were obtained using Wormbase (*C. elegans*) or NCBI BLAST (all other species). Top hits were imported into Geneious

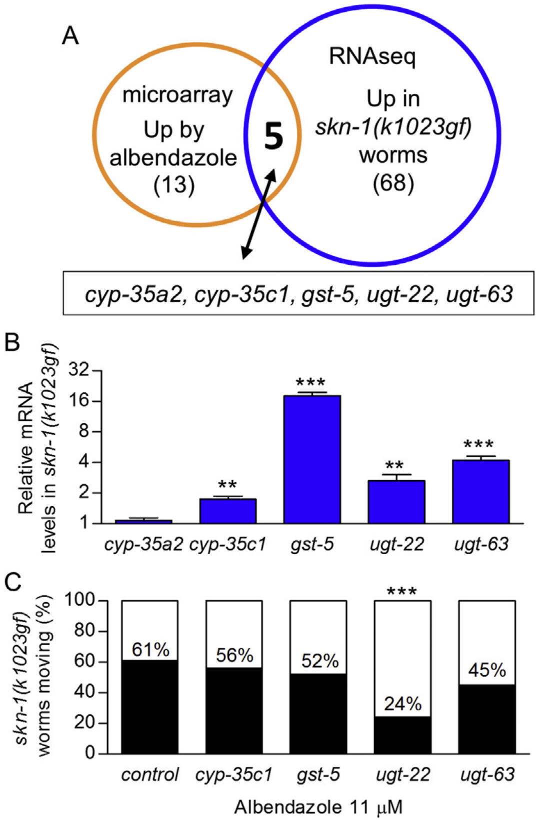

Fig. 3. *ugt-22* is induced in *skn-1(k1023gf)* worms. (A) Venn diagram of genes induced at least 2-fold in microarray data of 1.13 mM albendazole and RNAseq of *skn-1(k1023gf)* (*gf*, gain-of-function) worms (Laing et al., 2010; Peddibhotla et al., 2015). (B) Relative mRNA levels of the five overlapping genes in *skn-1(k1023gf)* worms (**$P < 0.01$; ***$P < 0.001$ relative to *wild type* worms (N2), $n = 3$–4 replicates of worms). (C) Percent long-term spontaneous motility of adult *skn-1(k1023gf)* worms fed *E. coli* HT115 expressing *control, cyp-35c1, gst-5, ugt-22, or ugt-63 dsRNA* and exposed to 11 μM albendazole for 3 days (***$P < 0.001$ relative to feeding with *control dsRNA* by Chi-square analysis, $n = 60$–187 worms).

version 6.1.8 and aligned using MAFFT version 7.017. Gaps were trimmed manually and alignments were imported into MEGA version 6 (Tamura et al., 2013). Phylogenic trees were generated by maximum likelihood using bootstraps with 500 replicates. Only branches with at least 50% bootstrap support are shown.

2.8. Statistical analysis, and reagent and data availability

Statistical significance was determined with Chi-square tests when number of motile versus immobile worms was compared. Non-linear regression curves were generated using a four-parameter dose-response regression in GraphPad Prism 5, after logarithmic ($\log_{10}$) transformation of the data. Bottom and top values were constrained to 0 and 100%, respectively. EC_{50} (effective concentration that inhibits motility in 50% of *C. elegans* worms) values were compared using the extra sum-of-squares *F*-test. T-tests were used to compare mRNA levels. *P* values of < 0.05 were considered to indicate statistical significance.

Strains are available upon request. Raw data used in the figures is available at: https://figshare.com/s/b03915fb6ebb525084d2.

3. Results

3.1. skn-1 gain-of-function increases long-term spontaneous motility in albendazole

The *skn-1(k1023gf)* gain-of-function allele is a missense mutation that renders SKN-1 constitutively active with 68 drug detoxification genes overexpressed at least two-fold as detected by RNAseq (Peddibhotla et al., 2015; Tang et al., 2015). To assess contributions of SKN-1 to benzimidazole efficacy, we grew *skn-1(k1023gf)* worms in the presence of the drug class representative albendazole from the L1 larval stage to adults and scored motility, a function severely impaired by the drug (Spence et al., 1982).

We initially quantified the effects of *skn-1(k1023gf)* mutation using a spontaneous motility assay. We filmed adult worms on agar plates for 1 min 45 s and counted the percentage that moved at least one worm body length. We used 11 μM when testing for increased motility, because this albendazole concentration reduces motility of *wild type* worms (N2) strongly (91%, Fig. 1A); we used 2.5 μM when testing for decreased motility, because this concentration reduces motility by only 35–50% (Figs. 1B and 4A).

We found that *skn-1(k1023gf)* worms are significantly more motile than *wild type* N2 worms when grown on 11 μM albendazole (Fig. 1A). Furthermore, *wild type* N2 worms appeared shorter than *skn-1(k1023gf)* worms on albendazole and maintained a curled body posture (Fig. 1C), two known morphological effects of benzimidazoles (Spence et al., 1982).

Mutations in *ben-1* confer strong resistance to benzimidazoles (Driscoll et al., 1989). We found no protein-changing mutations in *ben-1* cDNA in our previously published *skn-1(k1023gf)* RNAseq data (Peddibhotla et al., 2015). We also observed no decrease in *ben-1* mRNA levels in *skn-1(k1023gf)* worms (actually a slight increase) (Fig. S1) making it unlikely that unintended changes to BEN-1 are responsible for the effects observed in Fig. 1A and C.

3.2. skn-1 loss-of-function reduces long-term spontaneous motility in albendazole

We next tested if a *skn-1(zj15lf)* hypomorphic allele would decrease motility in albendazole; *skn-1(zj15lf)* is a point mutation near an exon boundary that causes RNA splicing errors, a 76% reduction in levels of the two long and stress-associated *skn-1* mRNA variants (i.e. *skn-1a* and *c*), and stress response phenotypes comparable to *skn-1(RNAi)* (Tang et al., 2015). Long-term spontaneous motility of *skn-1(zj15lf)* worms was 68% lower than *wild type* N2 in 2.5 μM albendazole ($p < 0.001$, Fig. 1B).

3.3. A rapid touch-response assay reveals shifts in albendazole EC50 values

To compare contributions of *skn-1* to albendazole resistance in multiple strains concurrently and over a broad range of concentrations, we used a higher throughput assay of motility that scores the percentage of worms able to elicit an immediate (within 1–2 s) backward withdraw in response to gentle touch with a thin hair to the side of the body near the posterior pharynx bulb (Chalfie and Sulston, 1981); this assay is similar to one used to originally characterize *ben-1* mutants (Driscoll et al., 1989) and used recently to score anthelmintic efficacy (Weaver et al., 2017). This response is robust, with essentially all worms in all strains responding when grown without albendazole (98–100%); this rapid touch-response is also more sensitive to the drug than spontaneous motility with full effectiveness at 5 μM albendazole in *wild type* N2 worms (Fig. 2A). We observed a statistically significant 1.7-fold increase in albendazole EC_{50} in *skn-1(k1023gf)* worms, and a 1.6-fold decrease in *skn-1(zj15lf)* worms compared to *wild type* N2 worms (Fig. 2A–B), confirming the role of *skn-1* over a range of concentrations. Importantly, *ben-1(e1880)* worms remained 100% motile at all

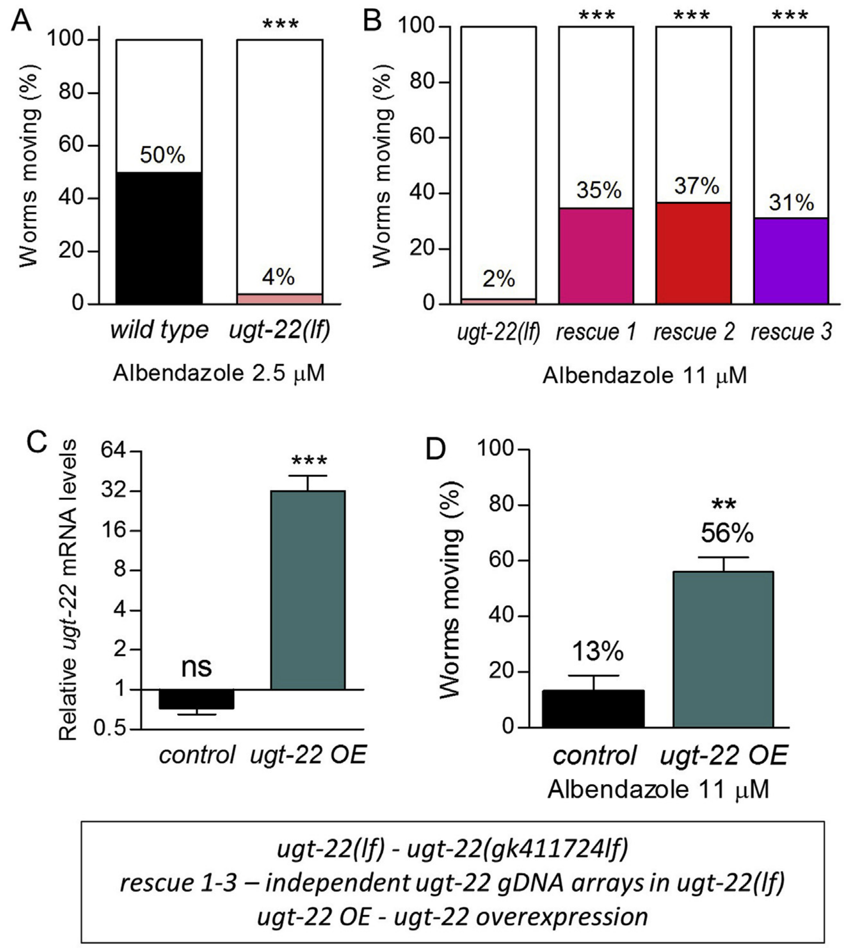

Fig. 4. *ugt-22* mutation and overexpression alter albendazole efficacy. (A) Percent long-term spontaneous motility of adult *wild type* (N2) and *ugt-22(gk411724lf)* (*lf*, loss-of-function) mutant worms exposed to 2.5 μM albendazole for 3 days. (B) Percent long-term spontaneous motility of three independently generated *ugt-22* gDNA extrachromosomal array lines in the *ugt-22(gk411724lf)* genetic background exposed to 11 μM albendazole for 3 days. Motility of all three *ugt-22* gDNA array lines was greater than *wild type* worms (N2) (9.4%) and comparable to *skn-1(k1023gf)* worms (40.5%) (values are from Fig. 1). (C) Relative mRNA levels of *ugt-22* in *control* and *ugt-22* transgenic lines. (D) Percent spontaneous motility of adult transgenic *control* and *ugt-22* overexpression (OE) lines exposed to 11 μM albendazole for 3 days. Motility of *ugt-22* overexpression transgenic lines was greater than *skn-1(k1023gf)* worms (40.5%) (value is from Fig. 1). $^{**}P < 0.01$, $^{***}P < 0.001$ relative to respective control worms; ns = not statistically significant. *n* = 79–278 worms per strain in (A–B) and three independent transgenic lines in (C–D) with 78–111 worms tested per line.

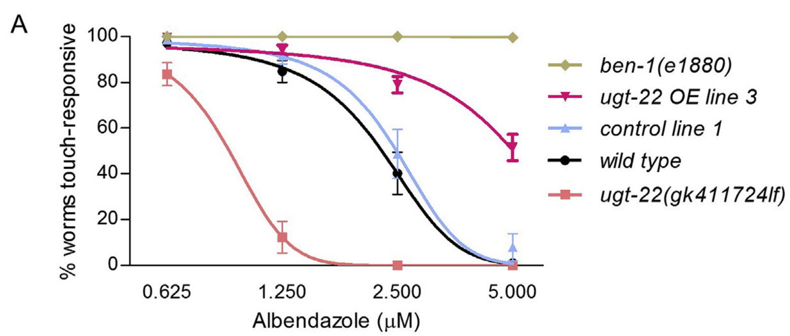

B

Strain	EC_{50}, [μM] (95% CI)	*P* value	Fold change of EC_{50} from *wild type*	R^2
ugt-22(gk411724lf)	0.86 (0.78-0.93)	<0.001	- 2.5	0.945
wild type	2.18 (1.93-2.47)	-	-	0.845
control line 1	2.47 (2.16-2.82)	0.228	1.1	0.915
ugt-22 OE line 3	5.14 (4.42-5.98)	<0.001	2.4	0.869

EC_{50} - 50% effective concentration
CI - confidence interval
OE - overexpression

Fig. 5. Albendazole dose-response curves are altered by *ugt-22* mutation and overexpression. (A) Percent rapid touch-responsive motility of adult *ugt-22(gk411724lf)* (*lf*, loss-of-function), *wild type* (N2), control line 1 (control transgenic array in a *wild type* background), *ugt-22* OE line 3 (*ugt-22* gDNA overexpression array in a *wild type* background), and *ben-1(e1880)* worms exposed to albendazole for 3 days. (B) EC_{50} values, *P*-values, and EC_{50} fold changes. Replicates equal 4–10 independent trials of ~20–50 worms per trial. Note that wild type and *ben-1* trials are the same in Fig. 2 and 5.

albendazole concentrations used (Fig. 2A) confirming that albendazole impairs this touch-response *via* actions on β-tubulin. The data in Figs. 1–2 demonstrate that genetic manipulation of *skn-1* changes albendazole efficacy in *C. elegans*.

3.4. The detoxification gene ugt-22 is associated with skn-1 gain-of-function

We next compared lists of detoxification genes that were previously shown to be induced by albendazole or *skn-1(k1023gf)* gain-of-function in microarray or RNAseq analyses, respectively (Laing et al., 2010; Peddibhotla et al., 2015) to identify candidates that may influence albendazole efficacy. Of the 13 predicted drug detoxification genes that were induced at least 2-fold by 1.13 mM albendazole (Laing et al., 2010), five overlap with the 68 predicted detoxification genes induced at least 2-fold in *skn-1(k1023gf)* (Fig. 3A) (Peddibhotla et al., 2015). Overlapping detoxification genes are the phase I detoxification cytochrome P450 family members *cyp-35a2* and *cyp-35c1* and the phase II detoxification genes *gst-5, ugt-22*, and *ugt-63*.

Using qPCR, we confirmed up-regulation of *cyp-35c1, gst-5, ugt-22,* and *ugt-63* in *skn-1(k1023gf)* worms (Fig. 3B). We tested the effect of RNAi for these four genes in *skn-1(k1023gf)* worms with the spontaneous motility assay on 11 μM albendazole. Only *ugt-22(RNAi)* reduced motility significantly (Fig. 3C). qPCR confirmed reduced mRNA levels for all four genes *(cyp-35c1, gst-5, ugt-22*, and *ugt-63)* in *skn-1(k1023gf)* worms, with *ugt-22(RNAi)* reducing *ugt-22* mRNA levels by 91.8% (Fig. S2A). These results suggest that *ugt-22* may influence albendazole efficacy.

3.5. Mutation and overexpression confirm the influence of ugt-22 on albendazole efficacy

To confirm the role of *ugt-22*, a *ugt-22(gk411724lf)* loss-of-function allele with a nonsense mutation at codon 89 of 534 total generated by the Million Mutation Project (Thompson et al., 2013) was outcrossed five times and tested for albendazole efficacy. qPCR indicates that this mutant produces a *ugt-22* mRNA that is likely degraded by the *C. elegans* non-sense mediated decay mechanism (Longman et al., 2008); *ugt-22* mRNA levels in *ugt-22(gk411724lf)* worms were reduced 94% relative to *wild type* worms (N2) (Fig. S2B), and any remaining mRNA would contain an early stop codon. In 2.5 μM albendazole, 50% of *wild type* N2 worms moved spontaneously at least one worm body length in 1 min 45 s (Fig. 4A); remarkably, only 4% of *ugt-22(gk411724lf)* worms moved at least one worm body length under these same conditions (Fig. 4A).

Three independent extra-chromosomal arrays containing a *ugt-22* genomic DNA PCR fragment were generated by injecting *ugt-22(gk411724lf)* worms and tested in the spontaneous motility assay (Fig. 4B). All three transgenic lines increased motility of *ugt-22(gk411724lf)* worms in 11 μM albendazole from 2% to 31–37% (Fig. 4B), which is above the mean for *wild type* worms (N2) (9.4%) and comparable to *skn-1(k1023gf)* worms (40.5%) (value is from Fig. 1A). In this experiment, each independent rescue line was compared to the single *ugt-22(gk411724lf)* parent worm strain.

We next generated three independent control and three independent *ugt-22* genomic DNA extra-chromosomal array lines in *wild type* worms (N2) to test the effects of extra *ugt-22* copies on their own. The control arrays had no effect on *ugt-22* mRNA levels, while the arrays containing *ugt-22* increased *ugt-22* mRNA levels by an average of 32.2 ± 9.8-fold ($p < 0.001$, Fig. 4C) relative to *wild type* worms (N2), confirming overexpression (OE) of *ugt-22*. These *ugt-22* overexpression arrays also increased long-term spontaneous motility on 11 μM albendazole to 56% compared to only 13% in the control lines ($p < 0.01$). This level of motility is above the mean for *skn-1(k1023gf)* worms (40.5%, value is from Fig. 1A); means were calculated from three independent lines, with at least three independent trials per line (Fig. 4D).

We used the rapid touch-response assay to compare contributions of *ugt-22* to albendazole resistance by comparing EC_{50} values of *wild type* worms (N2) with *ugt-22(gk411724lf)* worms and worms that overexpress *ugt-22;* we chose the overexpression line with the greatest increase in *ugt-22* mRNA levels (*ugt-22 OE line 3,* 43.1 ± 7.21, from Fig. 4C). Albendazole EC_{50} increased by 2.4-fold in the *ugt-22* overexpression worms and EC_{50} was decreased by 2.5-fold in *ugt-22(gk411724lf)* worms (Fig. 5A–B). Worms with the injection control (control line 1) were not different from *wild type* N2. *ben-1(e1800)* data are reshown from Fig. 2 for reference.

3.6. UGT-22 belongs to a rapidly evolving group of UGTs

We aligned *C. elegans* UGT-22 and putative UGT proteins from the parasites *Haemonchus contortus*, *Ascaris suum,* and *Brugia malayi* and humans that share highest protein sequence homology from BLAST searches. We found that core features of UGTs are shared (Fig. S3). These include the signal peptide, acceptor substrate binding pocket, donor binding region 1, donor binding region 2 (DBR2), and transmembrane domain. To explore UGT-22 homology, we first performed a maximum likelihood phylogenetic analysis of all putative *C. elegans* and human UGT proteins. *C. elegans* and human UGTs occupy different branches, consistent with lineage-specific gene duplication and UGT-22 not being a direct orthologue of any single human UGT (Fig. S4). A tree with UGT-22 homologs from *C. elegans* and three parasitic nematodes with annotated genomes demonstrates that UGT-22 groups within a large branch (80% bootstrap confidence levels) containing the majority of other *C. elegans* UGTs and seven *H. contortus* UGTs (Fig. S5). Together, these results show that UGT-22 homologs with similar amino acid features exist in a clade V intestinal parasite.

4. Discussion

Genetic analysis of parasitic nematode populations has confirmed selection for resistance alleles in genes orthologous to *ben-1* (Ghisi et al., 2007; Kwa et al., 1994; Silvestre and Cabaret, 2002). In our experiments, genetic manipulations of *skn-1* and *ugt-22* shifted albendazole EC_{50} by 1.6–2.5-fold in our touch-responsive motility assays (Figs. 2 and 5). This effect size is comparable to the ∼2-fold shift of thiabendazole EC_{50} reported recently for the nuclear receptor *nhr-176* and its downstream phase I detoxification gene *cyp-35d1* (Jones et al., 2015).

Based on conservation of key functional regions (Fig. S3), UGT-22 is predicted to be a UDP-glucosyltransferase (UGT), which are phase II detoxification enzymes that catalyze conjugation of glucose onto small hydrophobic molecules facilitating excretion (Ikushiro et al., 2004; Xu et al., 2013). Intact *C. elegans* and *H. contortus* were shown to glucosylate benzimidazoles, including albendazole (Jones et al., 2015; Laing et al., 2010; Vokral et al., 2013). Furthermore, increased benzimidazole glucosylation and total UGT activity are associated with resistance in parasitic nematodes (Vokral et al., 2012, 2013). It remains to be seen if UGT-22 directly catalyzes the conjugation of glucose onto albendazole and if homologous proteins have the same function in parasites. Similar to many other detoxification genes, mRNA levels of *ugt-22* were previously shown to be enriched in the intestine of *C. elegans* using cell sorting or tissue-specific mRNA binding proteins followed by transcriptomic analysis (Haenni et al., 2012; Lightfoot et al., 2016; Spencer et al., 2011).

Among nematode genomes that have been analyzed, drug detoxification and transporter gene family diversity generally matches potential exposure to xenobiotics from the environment through feeding on microbes. There is expansion in completely free-living bacteriophagous lineages such as *Caenorhabditis* and *Pristionchus* (Dieterich et al., 2008; Lindblom and Dodd, 2006; Zhao et al., 2007), reduction in completely parasitic lineages such as *Brugia* (Ardelli et al., 2010; Ghedin et al., 2007) and *Ascaris* (Jex et al., 2011), and intermediate gene family size in lineages such as *H. contortus* that have free-living and parasitic stages (Laing et al., 2013). There are 74 predicted *ugt* genes in *C. elegans* (Dieterich et al., 2008), 34 in *H. contortus* (Laing et al., 2013), 10 in *A. suum*, and only 1 in *B. malayi* (Lee et al., 2018). In our phylogenetic analysis of UGT proteins from four nematode species, the majority of *C. elegans* UGTs (44) grouped together on one branch (80% bootstrap support) that includes UGT-22, seven UGTs from *H. contortus*, but no proteins from *A. suum* or *B. malayi* (Fig. S5). Although the number of species in our analysis is small, this pattern is consistent with UGT-22 being related to a group of UGTs that is shared with the clade V parasite *H. contortus*. Given the large number of genes regulated by SKN-1 (Oliveira et al., 2009; Park et al., 2009; Peddibhotla et al., 2015), it is possible that other downstream detoxification genes could also contribute to albendazole resistance.

Identification of *ben-1* in *C. elegans* (Driscoll et al., 1989) was a critical step that led to a deeper understanding of benzimidazole resistance in parasites (Ghisi et al., 2007; Kwa et al., 1994; Silvestre and Cabaret, 2002). Unlike the case for β-tubulin, detoxification enzymes and regulatory genes are numerous, evolve rapidly, may function redundantly, and are likely to have specificity toward different drug class representatives (Dieterich et al., 2008; Lindblom and Dodd, 2006; Zhao et al., 2007). As a result, the molecular mechanisms of benzimidazole biotransformation are likely to be far more complex and nuanced than the simple target protein (β-tubulin) mechanism of action. Our results add to a growing list of studies implicating biotransformation enzymes and upstream regulators as potential factors in benzimidazole resistance in nematodes (Jones et al., 2015; Laing et al., 2010; Matouskova et al., 2016; Vokral et al., 2012, 2013). A complete understanding will likely require far more effort with systematic genetic screens for upstream regulators and downstream detoxification genes and translation of insights to parasitic species.

Acknowledgements

Some *C. elegans* strains were provided by the *Caenorhabditis* Genetics Center (CGC, University of Minnesota, Minneapolis, MN) supported by the National Institutes of Health Office of Research Infrastructure Programs (P40 OD010440). This work was supported by the National Science Foundation [grant numbers IOS-1120130 and IOS-1452948]. All experiments described in this paper were performed by PF. PF and KPC conceived the experiments, analyzed the data, and wrote the manuscript.

Appendix A. Supplementary data

Supplementary data related to this article can be found at http://dx.doi.org/10.1016/j.ijpddr.2018.04.006.

Conflicts of interest

Declarations of interest: none.

References

An, J.H., Blackwell, T.K., 2003. SKN-1 links *C. elegans* mesendodermal specification to a conserved oxidative stress response. Gene Dev. 17, 1882–1893.

Anderson, R., Truscott, J., Hollingsworth, T.D., 2014. The coverage and frequency of mass drug administration required to eliminate persistent transmission of soil-transmitted helminths. Philos. Trans. R. Soc. Lond. Ser. B Biol. Sci. 369, 20130435.

Ardelli, B.F., Stitt, L.E., Tompkins, J.B., 2010. Inventory and analysis of ATP-binding cassette (ABC) systems in *Brugia malayi*. Parasitology 137, 1195–1212.

Brenner, S., 1974. The genetics of *Caenorhabditis elegans*. Genetics 77, 71–94.

Caffrey, C.R., 2012. Parasitic Helminths: Targets, Screens, Drugs and Vaccines, Parasitic Helminths. Wiley-VCH Verlag GmbH & Co. KGaA, pp. I–XXIII.

Chalfie, M., Sulston, J., 1981. Developmental genetics of the mechanosensory neurons of *Caenorhabditis elegans*. Dev. Biol. 82, 358–370.

Choe, K.P., Leung, C.K., Miyamoto, M.M., 2012. Unique structure and regulation of the nematode detoxification gene regulator, SKN-1: implications to understanding and controlling drug resistance. Drug Metab. Rev. 44, 209–223.

Choe, K.P., Przybysz, A.J., Strange, K., 2009. The WD40 repeat protein WDR-23 functions with the CUL4/DDB1 ubiquitin ligase to regulate nuclear abundance and activity of SKN-1 in *Caenorhabditis elegans*. Mol. Cell Biol. 29, 2704–2715.

Dieterich, C., Clifton, S.W., Schuster, L.N., Chinwalla, A., Delehaunty, K., Dinkelacker, I., Fulton, L., Fulton, R., Godfrey, J., Minx, P., Mitreva, M., Roeseler, W., Tian, H., Witte, H., Yang, S.P., Wilson, R.K., Sommer, R.J., 2008. The *Pristionchus pacificus* genome provides a unique perspective on nematode lifestyle and parasitism. Nat. Genet. 40, 1193–1198.

Driscoll, M., Dean, E., Reilly, E., Bergholz, E., Chalfie, M., 1989. Genetic and molecular analysis of a *Caenorhabditis elegans* beta-tubulin that conveys benzimidazole sensitivity. J. Cell Biol. 109, 2993–3003.

Furtado, L.F., de Paiva Bello, A.C., Rabelo, E.M., 2016. Benzimidazole resistance in helminths: from problem to diagnosis. Acta Trop. 162, 95–102.

Garcia, C.M., Sprenger, L.K., Ortiz, E.B., Molento, M.B., 2016. First report of multiple anthelmintic resistance in nematodes of sheep in Colombia. An. Acad. Bras. Cienc. 88, 397–402.

Ghedin, E., Wang, S., Spiro, D., Caler, E., Zhao, Q., Crabtree, J., Allen, J.E., Delcher, A.L., Guiliano, D.B., Miranda-Saavedra, D., Angiuoli, S.V., Creasy, T., Amedeo, P., Haas, B., El-Sayed, N.M., Wortman, J.R., Feldblyum, T., Tallon, L., Schatz, M., Shumway, M., Koo, H., Salzberg, S.L., Schobel, S., Pertea, M., Pop, M., White, O., Barton, G.J., Carlow, C.K., Crawford, M.J., Daub, J., Dimmic, M.W., Estes, C.F., Foster, J.M., Ganatra, M., Gregory, W.F., Johnson, N.M., Jin, J., Komuniecki, R., Korf, I., Kumar, S., Laney, S., Li, B.W., Li, W., Lindblom, T.H., Lustigman, S., Ma, D., Maina, C.V., Martin, D.M., McCarter, J.P., McReynolds, L., Mitreva, M., Nutman, T.B., Parkinson, J., Peregrin-Alvarez, J.M., Poole, C., Ren, Q., Saunders, L., Sluder, A.E., Smith, K., Stanke, M., Unnasch, T.R., Ware, J., Wei, A.D., Weil, G., Williams, D.J., Zhang, Y., Williams, S.A., Fraser-Liggett, C., Slatko, B., Blaxter, M.L., Scott, A.L., 2007. Draft genome of the filarial nematode parasite *Brugia malayi*. Science (New York, N.Y.) 317, 1756–1760.

Ghisi, M., Kaminsky, R., Maser, P., 2007. Phenotyping and genotyping of *Haemonchus contortus* isolates reveals a new putative candidate mutation for benzimidazole resistance in nematodes. Vet. Parasitol. 144, 313–320.

Haenni, S., Ji, Z., Hoque, M., Rust, N., Sharpe, H., Eberhard, R., Browne, C., Hengartner, M.O., Mellor, J., Tian, B., Furger, A., 2012. Analysis of *C. elegans* intestinal gene expression and polyadenylation by fluorescence-activated nuclei sorting and 3'-end-seq. Nucleic Acids Res. 40, 6304–6318.

Hart, A.C., 2006. Behavior. In: WormBook : the Online Review of C. elegans Biology, pp. 1–67.

Holden-Dye, L., Walker, R.J., 2014. Anthelmintic drugs and nematicides: studies in Caenorhabditis elegans. In: WormBook : the Online Review of C. elegans Biology, pp. 1–29.

Ikushiro, S., Sahara, M., Emi, Y., Yabusaki, Y., Iyanagi, T., 2004. Functional co-expression of xenobiotic metabolizing enzymes, rat cytochrome P450 1A1 and UDP-glucuronosyltransferase 1A6, in yeast microsomes. Biochim. Biophys. Acta 1672, 86–92.

James, C.E., Davey, M.W., 2009. Increased expression of ABC transport proteins is associated with ivermectin resistance in the model nematode *Caenorhabditis elegans*. Int. J. Parasitol. 39, 213–220.

Janssen, I.J., Krucken, J., Demeler, J., von Samson-Himmelstjerna, G., 2013. *Caenorhabditis elegans*: modest increase of susceptibility to ivermectin in individual P-glycoprotein loss-of-function strains. Exp. Parasitol. 134, 171–177.

Jasmer, D.P., Goverse, A., Smant, G., 2003. Parasitic nematode interactions with mammals and plants. Annu. Rev. Phytopathol. 41, 245–270.

Jex, A.R., Liu, S., Li, B., Young, N.D., Hall, R.S., Li, Y., Yang, L., Zeng, N., Xu, X., Xiong, Z., Chen, F., Wu, X., Zhang, G., Fang, X., Kang, Y., Anderson, G.A., Harris, T.W., Campbell, B.E., Vlaminck, J., Wang, T., Cantacessi, C., Schwarz, E.M., Ranganathan, S., Geldhof, P., Nejsum, P., Sternberg, P.W., Yang, H., Wang, J., Wang, J., Gasser, R.B., 2011. *Ascaris suum* draft genome. Nature 479, 529–533.

Jones, L.M., Flemming, A.J., Urwin, P.E., 2015. NHR-176 regulates *cyp-35d1* to control hydroxylation-dependent metabolism of thiabendazole in *Caenorhabditis elegans*. Biochem. J. 466, 37–44.

Kamath, R.S., Martinez-Campos, M., Zipperlen, P., Fraser, A.G., Ahringer, J., 2001. Effectiveness of specific RNA-mediated interference through ingested double-stranded RNA in *Caenorhabditis elegans*. Genome Biol. 2 Research0002.

Keiser, J., 2015. Is *Caenorhabditis elegans* the magic bullet for anthelminthic drug discovery? Trends Parasitol. 31, 455–456.

Krucken, J., Fraundorfer, K., Mugisha, J.C., Ramunke, S., Sifft, K.C., Geus, D., Habarugira, F., Ndoli, J., Sendegeya, A., Mukampunga, C., Bayingana, C., Aebischer, T., Demeler, J., Gahutu, J.B., Mockenhaupt, F.P., von Samson-Himmelstjerna, G., 2017. Reduced efficacy of albendazole against *Ascaris lumbricoides* in Rwandan schoolchildren. Int. J. Parasitol. 7, 262–271 Drugs and drug resistance.

Kwa, M.S., Veenstra, J.G., Roos, M.H., 1994. Benzimidazole resistance in *Haemonchus contortus* is correlated with a conserved mutation at amino acid 200 in beta-tubulin isotype 1. Mol. Biochem. Parasitol. 63, 299–303.

Lacey, E., 1990. Mode of action of benzimidazoles. Parasitol. today 6, 112–115 (Personal ed.).

Laing, R., Kikuchi, T., Martinelli, A., Tsai, I.J., Beech, R.N., Redman, E., Holroyd, N., Bartley, D.J., Beasley, H., Britton, C., Curran, D., Devaney, E., Gilabert, A., Hunt, M., Jackson, F., Johnston, S.L., Kryukov, I., Li, K., Morrison, A.A., Reid, A.J., Sargison, N., Saunders, G.I., Wasmuth, J.D., Wolstenholme, A., Berriman, M., Gilleard, J.S., Cotton, J.A., 2013. The genome and transcriptome of *Haemonchus contortus*, a key model parasite for drug and vaccine discovery. Genome Biol. 14, R88.

Laing, S.T., Ivens, A., Laing, R., Ravikumar, S., Butler, V., Woods, D.J., Gilleard, J.S., 2010. Characterization of the xenobiotic response of *Caenorhabditis elegans* to the anthelmintic drug albendazole and the identification of novel drug glucoside metabolites. Biochem. J. 432, 505–514.

Lee, R.Y.N., Howe, K.L., Harris, T.W., Arnaboldi, V., Cain, S., Chan, J., Chen, W.J., Davis, P., Gao, S., Grove, C., Kishore, R., Muller, H.M., Nakamura, C., Nuin, P., Paulini, M., Raciti, D., Rodgers, F., Russell, M., Schindelman, G., Tuli, M.A., Van Auken, K., Wang, Q., Williams, G., Wright, A., Yook, K., Berriman, M., Kersey, P., Schedl, T., Stein, L., Sternberg, P.W., 2018 Jan 4. WormBase 2017: molting into a new stage. Nucleic Acids Res. 46 (D1), D869–D874.

Lewis, J.A., Wu, C.H., Berg, H., Levine, J.H., 1980. The genetics of levamisole resistance in the nematode *Caenorhabditis elegans*. Genetics 95, 905–928.

Lightfoot, J.W., Chauhan, V.M., Aylott, J.W., Rodelsperger, C., 2016. Comparative transcriptomics of the nematode gut identifies global shifts in feeding mode and pathogen susceptibility. BMC Res. Notes 9, 142.

Lindblom, T.H., Dodd, A.K., 2006. Xenobiotic detoxification in the nematode *Caenorhabditis elegans*. J. Exp. Zool. Comp. Exp. Biol. 305, 720–730.

Longman, D., Arrisi, P., Johnstone, I.L., Caceres, J.F., 2008. Chapter 7. Nonsense-mediated mRNA decay in *Caenorhabditis elegans*. Methods Enzymol. 449, 149–164.

Ly, K., Reid, S.J., Snell, R.G., 2015. Rapid RNA analysis of individual *Caenorhabditis elegans*. MethodsX 2, 59–63.

Matouskova, P., Vokral, I., Lamka, J., Skalova, L., 2016. The role of xenobiotic-metabolizing enzymes in anthelmintic deactivation and resistance in helminths. Trends Parasitol. 32, 481–491.

Oliveira, R.P., Porter Abate, J., Dilks, K., Landis, J., Ashraf, J., Murphy, C.T., Blackwell, T.K., 2009. Condition-adapted stress and longevity gene regulation by *Caenorhabditis elegans* SKN-1/Nrf. Aging Cell 8, 524–541.

Park, S.K., Tedesco, P.M., Johnson, T.E., 2009. Oxidative stress and longevity in *Caenorhabditis elegans* as mediated by SKN-1. Aging Cell 8, 258–269.

Peddibhotla, S., Fontaine, P., Leung, C.K., Maloney, P., Hershberger, P.M., Wang, Y., Bousquet, M.S., Luesch, H., Mangravita-Novo, A., Pinkerton, A.B., Smith, L.H., Malany, S., Choe, K., 2015. Discovery of ML358, a selective small molecule inhibitor of the SKN-1 pathway involved in drug detoxification and resistance in nematodes. ACS Chem. Biol. 10 (8), 1871–1879.

Pullan, R.L., Smith, J.L., Jasrasaria, R., Brooker, S.J., 2014. Global numbers of infection and disease burden of soil transmitted helminth infections in 2010. Parasites Vectors 7, 37.

Ramos, F., Portella, L.P., Rodrigues Fde, S., Reginato, C.Z., Potter, L., Cezar, A.S., Sangioni, L.A., Vogel, F.S., 2016. Anthelmintic resistance in gastrointestinal nematodes of beef cattle in the state of Rio Grande do Sul, Brazil. Int. J. Parasitol. 6, 93–101 Drugs and drug resistance.

Silvestre, A., Cabaret, J., 2002. Mutation in position 167 of isotype 1 beta-tubulin gene of Trichostrongylid nematodes: role in benzimidazole resistance? Mol. Biochem. Parasitol. 120, 297–300.

Soukhathammavong, P.A., Sayasone, S., Phongluxa, K., Xayaseng, V., Utzinger, J., Vounatsou, P., Hatz, C., Akkhavong, K., Keiser, J., Odermatt, P., 2012. Low efficacy of single-dose albendazole and mebendazole against hookworm and effect on concomitant helminth infection in Lao PDR. PLoS Neglected Trop. Dis. 6, e1417.

Spence, A.M., Malone, K.M.B., Novak, M.M.A., Woods, R.A., 1982. The effects of mebendazole on the growth and development of *Caenorhabditis elegans*. Can. J. Zool. 60, 2616–2623.

Spencer, W.C., Zeller, G., Watson, J.D., Henz, S.R., Watkins, K.L., McWhirter, R.D., Petersen, S., Sreedharan, V.T., Widmer, C., Jo, J., Reinke, V., Petrella, L., Strome, S., Von Stetina, S.E., Katz, M., Shaham, S., Ratsch, G., Miller 3rd, D.M., 2011. A spatial and temporal map of *C. elegans* gene expression. Genome Res. 21, 325–341.

Tamura, K., Stecher, G., Peterson, D., Filipski, A., Kumar, S., 2013. MEGA6: molecular evolutionary genetics analysis version 6.0. Mol. Biol. Evol. 30, 2725–2729.

Tang, L., Choe, K.P., 2015. Characterization of *skn-1/wdr-23* phenotypes in *Caenorhabditis elegans*; pleiotrophy, aging, glutathione, and interactions with other longevity pathways. Mech. Ageing Dev. 149, 88–98.

Tang, L., Dodd, W., Choe, K., 2015. Isolation of a hypomorphic *skn-1* allele that does not require a balancer for maintenance. G3 (Bethesda, Md.).

Thompson, O., Edgley, M., Strasbourger, P., Flibotte, S., Ewing, B., Adair, R., Au, V., Chaudhry, I., Fernando, L., Hutter, H., Kieffer, A., Lau, J., Lee, N., Miller, A., Raymant, G., Shen, B., Shendure, J., Taylor, J., Turner, E.H., Hillier, L.W., Moerman, D.G., Waterston, R.H., 2013. The million mutation project: a new approach to genetics in *Caenorhabditis elegans*. Genome Res. 23, 1749–1762.

Torgerson, P.R., Devleesschauwer, B., Praet, N., Speybroeck, N., Willingham, A.L., Kasuga, F., Rokni, M.B., Zhou, X.N., Fevre, E.M., Sripa, B., Gargouri, N., Furst, T., Budke, C.M., Carabin, H., Kirk, M.D., Angulo, F.J., Havelaar, A., de Silva, N., 2015. World Health Organization estimates of the global and regional disease burden of 11 foodborne parasitic diseases, 2010: a data synthesis. PLoS Med. 12, e1001920.

Vercruysse, J., Behnke, J.M., Albonico, M., Ame, S.M., Angebault, C., Bethony, J.M., Engels, D., Guillard, B., Nguyen, T.V., Kang, G., Kattula, D., Kotze, A.C., McCarthy, J.S., Mekonnen, Z., Montresor, A., Periago, M.V., Sumo, L., Tchuente, L.A., Dang, T.C., Zeynudin, A., Levecke, B., 2011. Assessment of the anthelmintic efficacy of albendazole in school children in seven countries where soil-transmitted helminths are endemic. PLoS Neglected Trop. Dis. 5, e948.

Vokral, I., Bartikova, H., Prchal, L., Stuchlikova, L., Skalova, L., Szotakova, B., Lamka, J., Varady, M., Kubicek, V., 2012. The metabolism of flubendazole and the activities of selected biotransformation enzymes in *Haemonchus contortus* strains susceptible and resistant to anthelmintics. Parasitology 139, 1309–1316.

Vokral, I., Jirasko, R., Stuchlikova, L., Bartikova, H., Szotakova, B., Lamka, J., Varady, M., Skalova, L., 2013. Biotransformation of albendazole and activities of selected detoxification enzymes in *Haemonchus contortus* strains susceptible and resistant to anthelmintics. Vet. Parasitol. 196, 373–381.

Weaver, K.J., May, C.J., Ellis, B.L., 2017. Using a health-rating system to evaluate the usefulness of *Caenorhabditis elegans* as a model for anthelmintic study. PLoS One 12, e0179376.

Xu, Z.S., Xue, W., Xiong, A.S., Lin, Y.Q., Xu, J., Zhu, B., Zhao, W., Peng, R.H., Yao, Q.H., 2013. Characterization of a bifunctional O- and N-glucosyltransferase from *Vitis vinifera* in glucosylating phenolic compounds and 3,4-dichloroaniline in *Pichia pastoris* and *Arabidopsis thaliana*. PLoS One 8, e80449.

Zhao, Z., Thomas, J.H., Chen, N., Sheps, J.A., Baillie, D.L., 2007. Comparative genomics and adaptive selection of the ATP-binding-cassette gene family in *Caenorhabditis species*. Genetics 175, 1407–1418.